Supporting Information

Construction of triazine polycarboxylate Co-MOF with flexible and rigid coordination arms as well as excellent catalytic reduction and adsorption properties

Min Liu[a], He Qun Cai[a], Shan Jiang[a], Yong Heng Xing[a*], Feng Ying Bai[a*]

[a]*College of Chemistry and Chemical Engineering, Liaoning Normal University, Dalian City 116029, P.R. China*

Corresponding author: xingyongheng2000@163.com (Prof. Yong Heng Xing), baifengying2003@163.com (Prof. Feng Ying Bai)

Supplementary Index

Materials and methods

All starting materials were of reagent grade quality and were obtained from commercial sources without further purification. The powder X-ray diffraction patterns (PXRD) of compound **1** was obtained on Advance-D8 equipped with Cu-Kα radiation, and the range was 5° <2θ <50°, with a step size of 0.02° (2θ) and a count time of 2 s per step at room temperature. All IR measurements were obtained using a Bruker AXS TENSOR-27 FT-IR spectrometer with pressed KBr pellets in the range of 400–4000 cm^{-1} at room temperature. UV-vis-NIR spectra were recorded on a JASCO V-570 UV/vis/NIR microspectrophotometer (200-2500 nm). Liquid UV-visible absorption spectroscopy was performed on SPECORD 250/PLUS. The maximum absorption wavelength of the PNP solution was measured on spectrophotometer UV-1000. Meanwhile, the maximum absorption wavelength of iodine in cyclohexane solution was recorded on spectrophotometer UV-1000. Thermogravimetric analysis (TG) was performed on a PerkinElmer Diamond TG/DTA under N_2 atmosphere from 30 °C to 800 °C with a heating rate of 10 °C/min. The N_2 adsorption–desorption isotherms and the pore size were conducted using the Autosorb-IQ-XR Gas Sorption Analyzer (Quantachrome, Florida, USA) with the Brunauer-Emmet-Teller (BET) method at the liquid nitrogen temperature, respectively. The ^{1}H-NMR spectrum was performed on Bruker Avance II 400 Nuclear Magnetic Resonance Spectrometer (Bruker, Karlsruhe, Germany).

X-ray crystallographic determination

Single crystals of compound **1** was mounted on glass fibers for X-ray measurement. Reflection data was collected at room temperature on a Bruker AXS SMART APEX II CCD diffractometer with graphite monochromatized Cu-Kα radiation (λ = 1.54178 Å). All the measured independent reflections (I > 2σ (I)) were used in the structural analyses, and semi-empirical absorption corrections were applied using the SADABS program[1]. All calculations were performed in OLEX-2 platform[2,3]. The crystal was kept at 100 K during data collection. During the crystal resolution of compound **1**, we used OMIT instructions to remove Bad Reflections in the structure. SQUEEZE the diffraction peaks of the disordered guest molecules of

the compound **1** using PLATON software. The results show that there are 112 electrons in each structural unit of the compound **1.** According to the calculation result of SQUEEZE, including two point five free DMF and half free H_2O were directly added to the final molecular formula of the compound, and it was verified by elemental analysis and thermogravimetric analysis. Compound **1** was crystallized using a uniaxial diffractometer, and we made various attempts to grow better quality crystals without success. In the meantime, we have tested the SCXRD structural data of compound **1** for several times at low temperature, unfortunately, it is found that it is currently the best testing data. So, compound **1** have alert B of Checkcif, PLAT420_ALERT_2_B: These issues of alert level B possibly result from the solvent molecules are highly disordered.

Synthesis of ligand H_6BATD and compound 1

Synthesis of 5, 5'-((6-biscarboxymethylamino-1, 3, 5-triazine-2, 4-diyl) bis (azadiyl) (H_6BATD). The specific synthesis is as follows: add 5-aminoisophthalic acid (9.1 g, 50 mmol), NaOH (5M 19 mL) and $NaHCO_3$ (4.6 g, 55 mmol) to 100 mL H_2O into a three-necked flask. The mixture was stirred at 0 ºC for 10 min, followed by dropwise addition of cyanuric chloride (4.6 g, 25 mmol) in acetone (25 mL). After the dropwise addition, the mixture was stirred at 25 °C for 10 min, heated and stirred in a water bath at 45 °C for 3.5 h, and stirred at 25 °C for 16 h. After stirring at 25 °C, the solution was rotary evaporated to half the volume of the mother liquor and filtered with suction. 150 mL of ethanol was added to the obtained solution, and a white precipitate was precipitated, which was filtered off with suction. The solid in the upper filter cake was washed repeatedly with ethanol and air-dried to obtain the intermediate.

All the obtained intermediates were dissolved in 100 ml of deionized water, and 3.2 g (24 mmol) of iminodiacetic acid and 6.0 g (72.0 mmol) of $NaHCO_3$ were added respectively, and a magnet was added to fully stir and dissolve, and refluxed at 100 °C for 16 h. Suction filtration after cooling. 6 M hydrochloric acid was added dropwise to the obtained liquid to pH ≈ 2 and kept stirring to obtain a white precipitate, filtered, washed with deionized water until neutral, and dried to obtain 13.7 g of product H_6BATD (the yield was 88.3%). ^{1}HNMR (500 MHz, DMSO-d_6): δ 12.84 (s, 2H),

9.65 (s, 1H), 8.52 (s, 2H), 8.05 (s, 2H), 4.38 (s, 2H). The ^{1}H NMR spectrum of the ligand H_6TDPAT is shown in Fig. S1. The specific synthesis route was shown in Scheme S1.

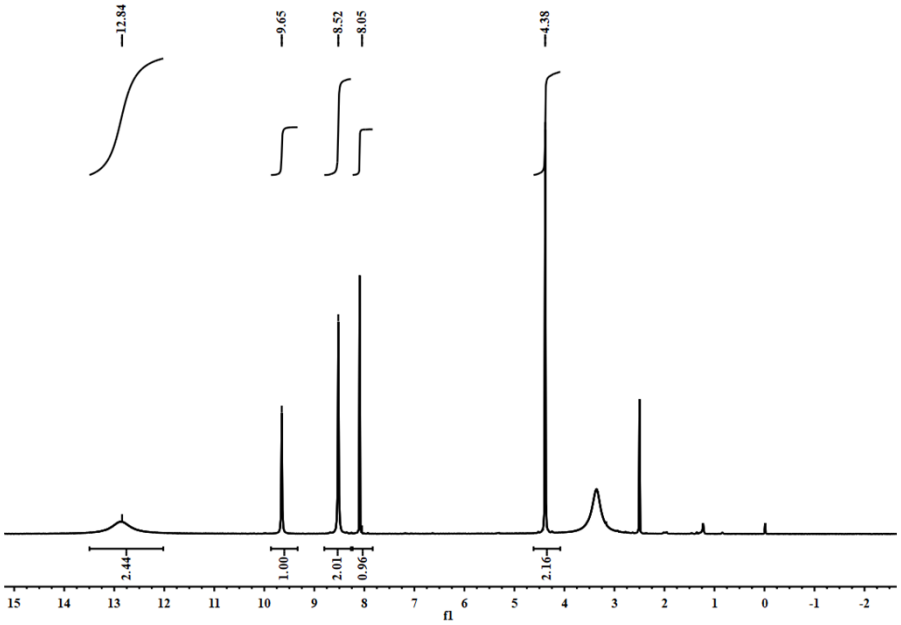

Figure S1 ^{1}HNMR spectrum of the H_6BATD ligand.

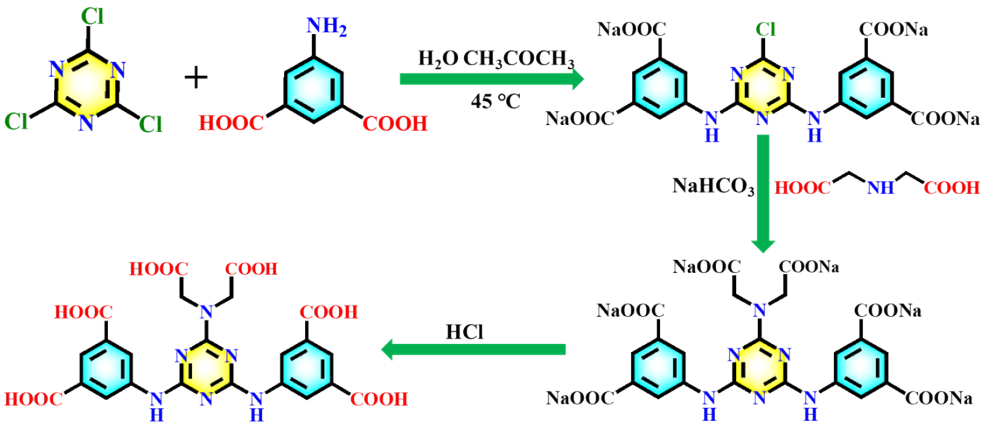

Scheme S1 Synthesis route of H_6BATD ligand.

Synthesis of compound 1

A mixture containing $Co(NO_3)_2 \cdot 6H_2O$ (10.2 mg 0.04 mmol) and H_6BATD (11.4 mg, 0.02 mmol) was dissolved in 2 mL DMF, 0.2 mL of H_2O and 0.5 mL of EtOH. Next, it was stirred at room temperature for 1 h, the mixed solution was sealed in a high temperature resistant glass bottle and heated in an oven at 100 °C for 48 h. After cooling to room temperature, the collected needle pink crystals were washed with DMF and dried naturally.

$[Co_2(H_2BATD)(DMF)_2]\cdot 2.5DMF\cdot 0.5H_2O$: (**1**) Yield: 67% (based on Co (II)), Elemental analysis $C_{36.5}H_{46.5}N_{10.5}O_{17}Co_2$ measured value (%): C, 42.76; H, 4.91; N, 14.73 ; theoretical value (%): C, 42.47; H, 4.51; N, 14.26. Infrared spectrum (KBr, cm^{-1}): 3417, 2938, 1650, 1380, 1059, 880.

Table S1. Crystal data and structure refinement for the compound **1**

Compound **1**	
Chemical formula	$C_{29}H_{29}N_8O_{14.5}Co_2$

M ($g \cdot mol^{-1}$)	839.46
Crystal system	monoclinic
Space group	*C*2/*c*
a (Å)	29.1298(6)
b (Å)	16.4226(4)
c (Å)	20.0583(4)
α (deg)	90
β (deg)	104.196(2)
γ (deg)	90
V (Å³)	9302.6(4)
Z	8
$\rho_{calc}(g \cdot cm^{-3})$	1.199
F (000)	3432.0
$\mu\ (mm^{-1})$	6.125
2θ (deg)	6.226 to 151.634
Reflections collected	29258
Independent reflections (I>2σ(*I*))	9317
Parameters	490
$\Delta(\rho)\ (e\ Å^{-3})$	-1.55
Goodness of fit on F^2	1.095
R^{α}	0.0870 (0.1035)[b]
wR_2^{α}	0.2583 (0.2834)[b]

*[a]$R=\sum \left| F_O-F_C \right| / \sum \left| F_O \right|$, $wR_2=\{\sum[w(F_O^2-F_C^2)^2]/\sum[w(F_O^2)^2]\}^{1/2}$; $[F_O>4\sigma(F_O)]$. [b]Based on all data.

Table S2. The selected bond distances (Å) and angles (°) of compound **1**

Compound **1**			
Co(1)-O(4)$^{\#1}$	2.103(3)	Co(1)-O(2)	2.071(3)

Co(1)-O(14)$^{\#2}$	2.109(4)	Co(1)-O(11)$^{\#3}$	2.108(4)
Co(1)-O(7)$^{\#3}$	2.082(3)	Co(1)-O(1)	2.136(4)
Co(2)-O(6)	1.976(4)	Co(2)-O(3)$^{\#3}$	2.039(4)
Co(2)-O(13)$^{\#4}$	2.028(4)	Co(2)-O(8)	2.151(4)
Co(2)-O(10)$^{\#3}$	2.007(4)	O(4)$^{\#1}$-Co(1)-O(14)$^{\#2}$	94.27(13)
O(4)$^{\#1}$-Co(1)-O(11)$^{\#3}$	100.76(13)	O(4)$^{\#1}$-Co(1)-O(1)	83.30(14)
O(2)-Co(1)-O(4)$^{\#1}$	85.43(13)	O(2)-Co(1)-O(14)$^{\#2}$	91.78(15)
O(2)-Co(1)-O(11)$^{\#3}$	173.77(13)	O(2)-Co(1)-O(7)$^{\#3}$	92.74(13)
O(2)-Co(1)-O(1)	89.94(15)	O(14)$^{\#2}$-Co(1)-O(11)$^{\#3}$	88.47(13)
O(14)$^{\#2}$-Co(1)-O(1)	176.91(14)	O(11)$^{\#3}$-Co(1)-O(1)	90.09(16)
O(7)$^{\#3}$-Co(1)-O(4)$^{\#1}$	165.76(15)	O(7)$^{\#3}$-Co(1)-O(14)$^{\#2}$	99.90(14)
O(7)$^{\#3}$-Co(1)-O(11)$^{\#3}$	81.09(14)	O(7)$^{\#3}$-Co(1)-O(1)	82.58(15)
O(6)-Co(2)-O(3)$^{\#3}$	95.64(16)	O(6)-Co(2)-O(13)$^{\#4}$	152.13(16)
O(6)-Co(2)-O(8)	88.85(17)	O(6)-Co(2)-O(10)$^{\#3}$	109.68(19)
O(3)$^{\#3}$-Co(2)-O(8)	175.19(17)	O(13)$^{\#4}$-Co(2)-O(3)$^{\#3}$	93.24(17)
O(13)$^{\#4}$-Co(2)-O(8)	81.97(19)	O(10)$^{\#3}$-Co(2)-O(3)$^{\#3}$	93.79(17)
O(10)$^{\#3}$-Co(2)-O(13)$^{\#4}$	95.99(19)	O(10)$^{\#3}$-Co(2)-O(8)	86.30(19)
C(25)-O(4)-Co(1)$^{\#1}$	141.7(3)	C(26)-O(3)-Co(2)$^{\#3}$	134.5(3)

*Symmetry codes: For compound **1**: #1:3/2-x, 1/2-y, 1-z; #2: 1/2+x, 1/2-y, 1/2+z; #3: 1-x, 1-y, 1-z; #4: 1/2-x, 1/2+y, 1/2-z.

Detailed description of the experiment process

(1) Catalytic reduction of PNP

The solution of PNP (0.10 mM, 40 mL) and a solution of KBH_4 (0.2 M, 2mL) was prepared. When the solutions were stirred and mixed, it was found that the color changed from light yellow to bright yellow. Then we added compound **1** to the

reaction system and recording the spectral changes of PNP (400 nm) by UV-vis spectrometer. To further calculate the catalytic reduction rate, we prepared a standard curve for PNP, as shown in Fig. S2a. Through the curves of PNP measured at different concentrations (0.025 mM-0.15 mM), we obtained the conversion relationship between concentration and absorbance. Monitoring the spectral changes of PNP (400 nm), equation 1 was used to calculate the catalytic reduction rate *R%*.

$$R\% = (C_0 - C_t)/C_0 \times 100 \qquad (1)$$

Where *R%* represents the catalytic reduction rate of the PNP, C_0 (mM) represents the initial concentration of the PNP, and C_t (mM) represents the concentration of the PNP at a certain time.

(2) Adsorption of iodine solution in cyclohexane

Volatile iodine readily dissolves in cyclohexane solution and is harmful to environmental pollution. In this work, 200 ppm iodine cyclohexane solution was prepared to explore the iodine adsorption capacity of the compounds. Different doses (20, 30, 40, and 60 mg) of the compound **1** was respectively soaked in cyclohexane solution of iodine (10 mL 200 ppm) at 25 °C. We recorded the adsorption of iodine by compound **1** as an adsorbent in cyclohexane solution (522 nm) by UV-vis spectrophotometer, and the characteristic peak of iodine in cyclohexane solution gradually decreased with time. To further calculate the removal rate, we prepared a standard curve for iodine in cyclohexane solution, as shown in Fig. S2b. Different concentrations of iodine in cyclohexane solution (25-200 ppm) were measured, and we obtained the conversion relationship between the concentration of iodine in cyclohexane solution and the absorbance. The removal rate *E%* was calculated using equation 2 by monitoring the spectral changes of iodine in cyclohexane (522 nm).

$$E\% = (C_0 - C_t)/C_0 \times 100 \qquad (2)$$

Where *E%* represents the removal rate of the iodine in cyclohexane, C_0 (ppm) represents the initial concentration of the iodine in cyclohexane, and C_t (ppm) represents the concentration of the iodine in cyclohexane at a certain time.

(3) Desorption curves of iodine in EtOH

In order to explore the reusability of compound **1**, we carried out a continuous

cycle experiment. At the end of each cycle, the adsorbent was filtered out and put into ethanol solution for desorption experiments. Similarly, in order to conveniently calculate the desorption rate of iodine in cyclohexane solution, we prepared a series of 10 mL ethanol solutions of iodine with different concentrations, and measured the corresponding absorbance with a UV-vis spectrophotometer. Taking the concentration of iodine in ethanol solution (5-50 ppm) and absorbance (Abs) as the abscissa and ordinate, respectively. As shown in Fig. S2c, we obtain a standard curve of the relationship between the concentration of iodine in ethanol solution and absorbance.

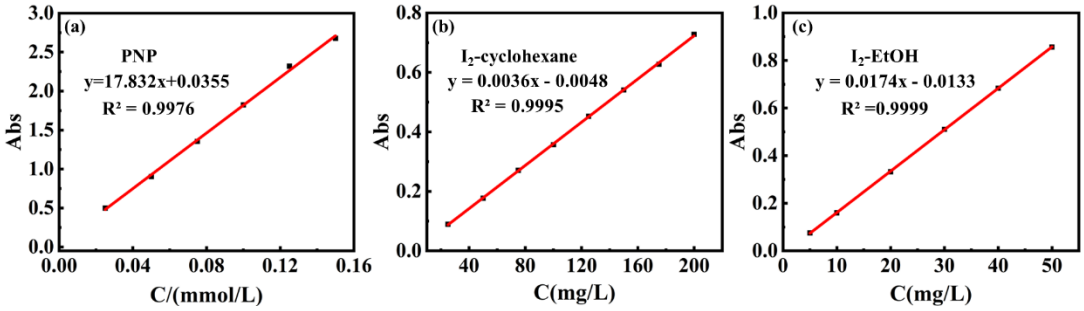

Figure S2 Standard curve: (a) PNP; (b) I_2-cyclohexane; (c) I_2-EtOH.

IR spectra:

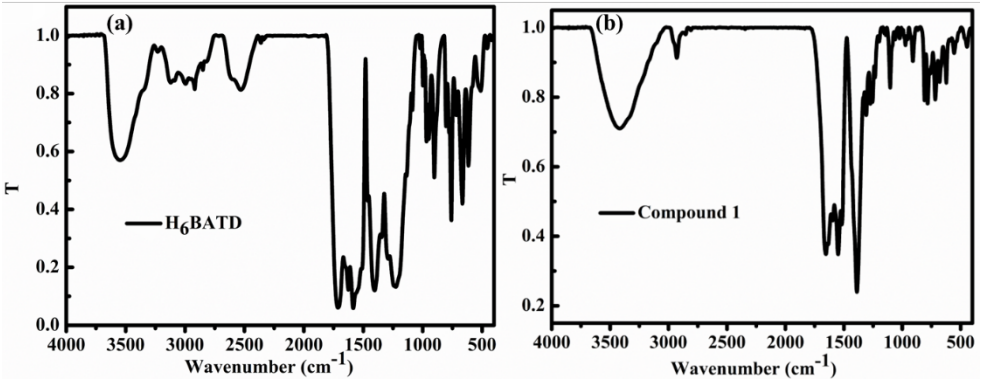

Figure S3 IR spectra: (a) H_6BATD; (b) compound **1**

Table S3 IR spectra (cm^{-1}) of H_6BATD and compound **1**

	H_6BATD	Compound **1**
ν_{OH}	3544	3417
ν_{C-H}	3116	3095
ν_{NH}	3108	2938
$\nu_{as(COO)^-}$	1719, 1588	1650, 1557
$\nu_{s(COO)-}$	1418	1380
ν_{C-N}	1084	1059
δ_{Ar-H}	901, 778	880, 765

UV-vis spectra:

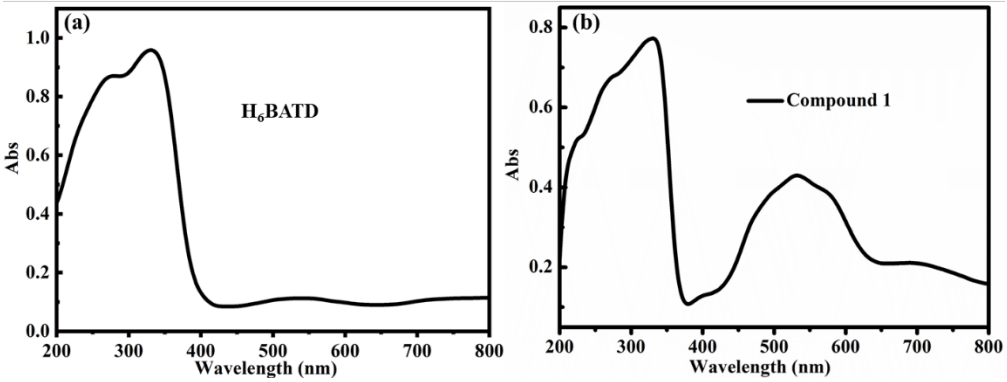

Figure S4 UV-vis spectra: (a) H_6DPOT; (b) Compound **1**

Table S4 UV spectra (nm) of H_6BATD, compound **1**

	Wavelength(nm)	Transition	Types
H_6BATD	272	π-π*	LLCT
	331	n-π*	LLCT
Compound **1**	274	π-π*	LLCT
	337	n-π*	LLCT
	402	O→Co	LMCT
	532, 704, 750	d-d*	MMCT

PXRD

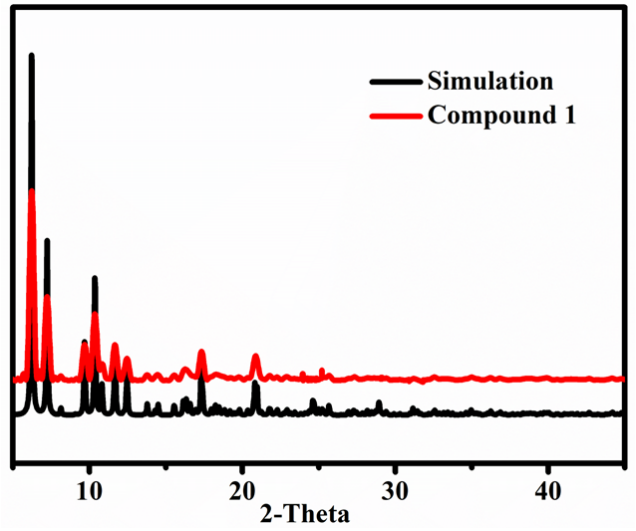

Figure S5 PXRD pattern of compound **1**

TG curve

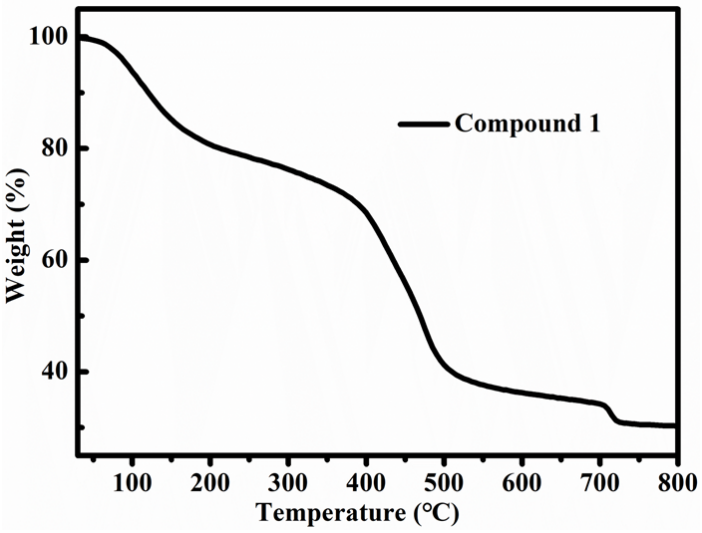

Figure S6 Thermal curve of compound **1**

Table S5 TG analysis of compound **1**

Compound		The first stage of weightlessne	The second stage of weightlessness	The third stage of weightlessn	Residue
1	Temperature (°C)	86-219	258-412	430-800	CoO
	Weightlessness designation	0.5 H_2O, 2.5 DMF	2 DMF	Partial collapse	
	Actual weightlessness (%)	17.38%	11.27%	32.5%	
	Theoretical weight loss rate (%)	18.59%	12.81%	30.6%	

BET surface area

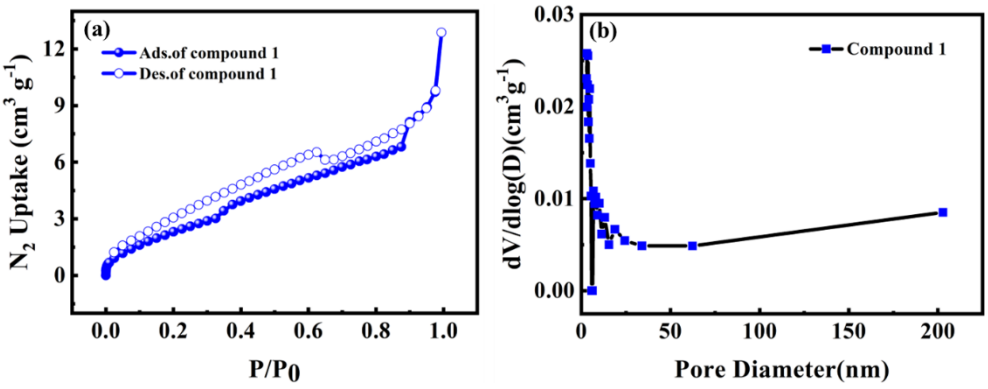

Figure S7 Compound **1**: (a) Nitrogen sorption isotherms; (b) Pore diameter distributions

IR spectra before and after catalytic PNP

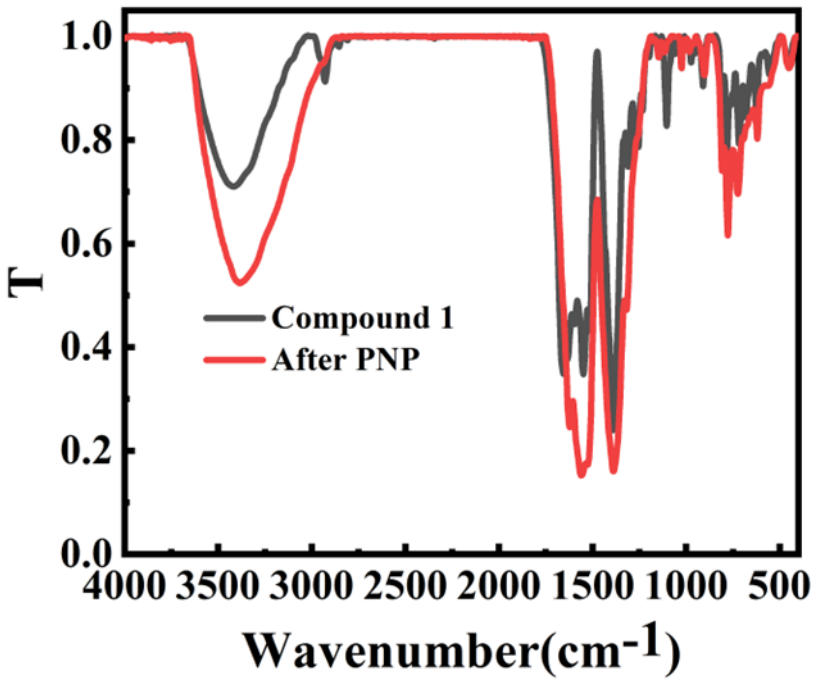

Figure S8 IR spectra before and after catalytic PNP

Pseudo-first-order kinetic equation

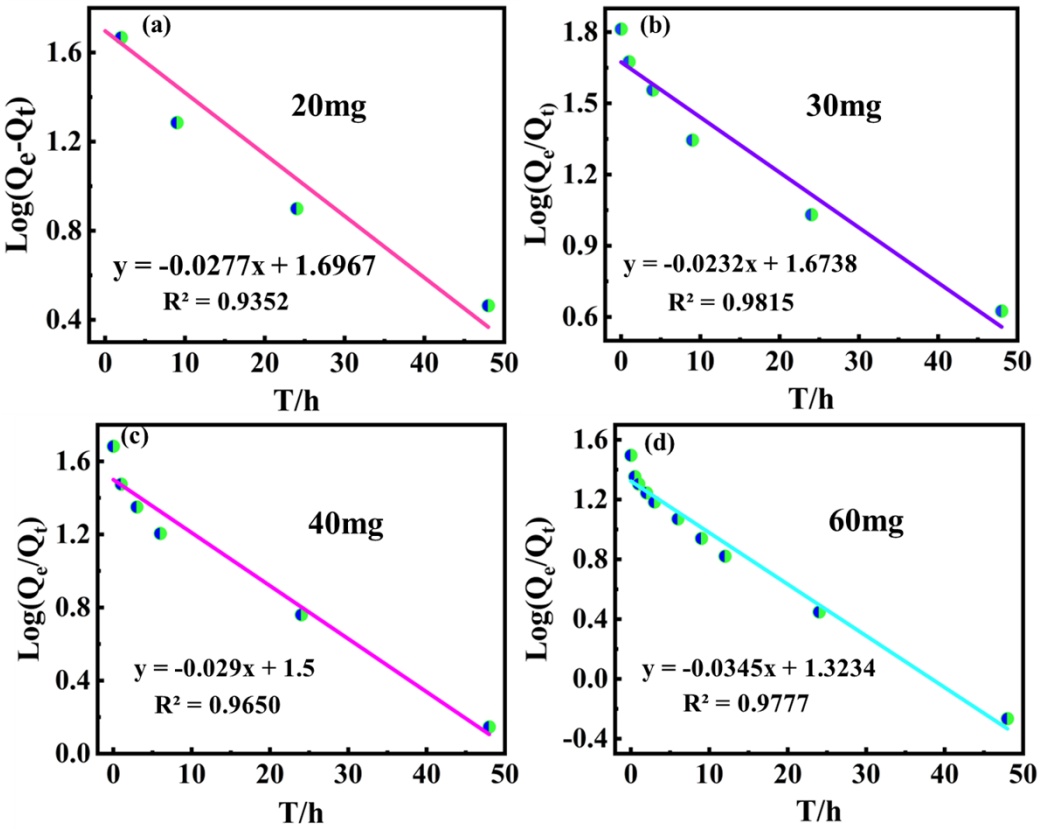

Figure S9 Pseudo-first-order kinetic model of compound **1**

References

[1] SMART and SAINT (software packages); Siemens Analytical X-ray Instruments,

Inc.: Madison, WI, 1996.

[2] O. V. Dolomanov，L. J. Bourhis，R. J. Gildea，J. Howard，H. Puschmann, *Journal of Applied Crystallography*, 2009, **42**, 339-341.

[3] G. M. Sheldrick, *Acta Crystallographica*, 2015, **71**, 3-8.